Computer Systems Science & Engineering
DOI: 10.32604/csse.2023.030393
Article

Tech Science Press

BE-RPL: Balanced-load and Energy-efficient RPL

S. Jagir Hussain* **and M. Roopa**

Department of Electronics and Communication Engineering, SRM Institute of Science and Technology, Ramapuram, Chennai, India
*Corresponding Author: S. Jagir Hussain. Email: js4534@srmist.edu.in
Received: 25 March 2022; Accepted: 04 May 2022

Abstract: Internet of Things (IoT) empowers imaginative applications and permits new services when mobile nodes are included. For IoT-enabled low-power and lossy networks (LLN), the Routing Protocol for Low-power and Lossy Networks (RPL) has become an established standard routing protocol. Mobility under standard RPL remains a difficult issue as it causes continuous path disturbance, energy loss, and increases the end-to-end delay in the network. In this unique circumstance, a Balanced-load and Energy-efficient RPL (BE-RPL) is proposed. It is a routing technique that is both energy-efficient and mobility-aware. It responds quicker to link breakage through received signal strength-based mobility monitoring and selecting a new preferred parent reactively. The proposed system also implements load balancing among stationary nodes for leaf node allocation. Static nodes with more leaf nodes are restricted from participating in the election for a new preferred parent. The performance of BE-RPL is assessed using the COOJA simulator. It improves the energy use, network control overhead, frame acknowledgment ratio, and packet delivery ratio of the network.

Keywords: COOJA simulator; energy; handover; internet of things; BE-RPL; load balancing; low-power and lossy network; mobility; routing protocols; RPL

1 Introduction

Because of high-level improvements in embedded devices and data connection protocols, the Internet of Things has developed as a key technology [1].

Wireless Sensor Networks (WSN) are comparable to mobile ad hoc networks in that they are susceptible to security threats [2,3]. WSN devices are connected to the Internet via the 6LowPAN invention. It allows even small devices to connect to the IP network. In terms of limited computing power, energy consumption, and memory, WSN devices are asset-obsessed [4]. High loss rates, poor data rates, and inconsistency result from the interconnection of asset-obsessed devices [5]. Industrial automation, smart buildings, smart education, medical assistance, health monitoring, and senior care are just a few of the applications for these Low-power and Lossy networks [6–9].

We concentrated on the healthcare domain in this article in order to simplify various medical activities and assist clinicians in monitoring their patients' health regardless of their location. Hosting a healthcare application necessitates managing the associated devices' mobility. Patients have implanted wireless

sensing devices that transmit data in real time during clinical monitoring. Patients are mobile nodes that create traffic and move freely while being connected to the infrastructure of stationary nodes. In an IP-based architecture, traditional LLN routing methods are not desirable [10]. Despite the fact that many distinct protocols have been established, interoperability concerns on the Internet have arisen. The Internet Engineering Task Force (IETF) created the Routing Protocol for Low-Power and Lossy Networks to address this issue. RPL was created to match the requirements of the 6LowPAN adaption layer, making it suitable for LLN routing. The focus of this research is on micro-mobility, which occurs when nodes move within a network without altering their addresses. The disappearance of nodes when they run out of charge or move is the main concern in LLN [11,12]. To deal with such issues, RPL provides local and global repair procedures [13].

The process of local repair is reactive. When a node detaches from its preferred parent, data is lost until a new parent node can be discovered and interfaced with. This has an impact on network performance. The mobility problem is addressed by the global repair mechanism, which restores the routing tree worldwide. When a single node vanishes, this strategy ends up being unproductive because it recreates the entire routing tree.

We propose a well-defined, Balanced-load and Energy-efficient RPL protocol to address these challenges experienced by RPL. It monitors node mobility and initiates handover procedures reactively. BE-RPL also considers load balancing across static nodes when choosing a new preferred parent.

The suggested system is unique in that

- It selects a legitimate set of nodes based on load (the number of attached child nodes).
- Based on the Received Signal Strength Indicator (RSSI) and residual energy, preferred parent selection among chosen static nodes.

The remainder of this work is organized in the following manner. In Section 2: fundamentals of standard RPL and its concern with mobile nodes are covered. Section 3: discusses relevant works and their issues. Section 4: delves into the terminologies, control packets, and timings involved with BE-RPL. BE-RPL is covered in full in Section 5. Section 6: Simulation and analysis of the results. Section 7 contains Conclusion.

2 RPL Basics and Mobility Issue

The DODAG (Destination Oriented Directed Acyclic Graph) [14] is used in the RPL routing tree. The RPL supports multipoint-to-point, point-to-multipoint, and point-to-point communications [15]. Building a DODAG is based on goals [16]. To keep track of topology, the RPL employs four distinct IDs. A rank is assigned to each node in the network. The rank is determined by the node's distance from the DODAG root, the goal function, and the metrics. In the upward direction, rank strictly reduces, while in the downward direction, rank strictly increases.

RPL introduces following ICMPv6 control messages: DODAG Information Object (DIO), DODAG Information Solicitation (DIS), Destination Advertisement Object (DAO), and DAO Acknowledgement (DAO-ACK). The root node is the first to transmit DIO. Nodes that get this DIO track down their preferred parent (PP) node and join as leaf nodes [17]. After discovering PP, every node predicts its position. Then it reconstructs the DIO and broadcasts it. This cycle proceeds till each node in the topology joins the DODAG. The DIS message is used to demand DIO messages from neighbors. A DAO control message is utilised to enable downward traffic. DAO-ACK acknowledges the received DAO.

In DODAG, node mobility causes inconsistency. There is no mobility identification in RPL. It does not distinguish between fixed and mobile nodes. RPL uses the trickle timer algorithm or the IPv6 Neighbour Discovery approach to detect topology changes. RPL employs a local or global repair technique to address the discrepancy after detecting network topology changes. When a node detects a link failure and

has no alternative parent, the local repair is immediately begun to discover an alternate path or parent. When a node leaves DODAG, it announces INFINIT RANK as its rank to alert its sub DODAG. Then it connects to DODAG by finding a new preferred parent node. The network's shape may change as a result of this repair approach, necessitating the rebuilding of the DODAG. This is accomplished through the employment of a global repair mechanism. This process is started by the DODAG root altering the DODAG Version Number, resulting in a new DODAG. This global repair brings about critical control traffic in the network. Both the repair mechanisms are reactive in nature and respond after node detachment. During this detachment, data loss occurs, which affects the network performance.

3 Related Work and Issues

We briefly cover some research related to RPL under node mobility circumstances in this section. The authors of [18] talk about RPL mobility possibilities in a VANET. To accommodate frequent topology changes, they deactivate the DIO trickle timer. Second, they recommended that the routing graph be updated by evaluating link quality. To prevent loop difficulties, they also included parent IDs in DIO messages.

The authors suggested GI-RPL [19] as a VANET alternative to RPL. To deal with frequent changes in topology, localization strategies were adopted. They presented an adjustable DIO period that improves performance by increasing the packet delivery ratio and decreasing packet latency. In GI-RPL, energy restrictions were not taken into account.

In [20], the authors suggested Mobility Enhanced RPL (MERPL). The stability of the route was improved by selecting a static node as the preferred parent. Mobile node disconnection was avoided by sending DIS messages on a regular basis in order to request DIO messages, which were subsequently used to re-join during the disconnection. Handover latency, signalling cost, and energy usage were not taken into account by MERPL.

In [21], the authors suggested mRPL. mRPL predicts node migration using the RSSI and employs a smart-HOP mechanism to handoff mobile node connections to new PP nodes. The overhead of control messages and energy usage are not taken into account.

Mobile nodes are in charge of initiating handoff techniques while changing positions in the majority of the above solutions. In general, mobile nodes have fewer resources. Because mobile nodes have restricted capabilities, other nodes, known as parent nodes, must offer a way to handle mobility. The parent node is intended to have greater resources, such as battery power, bandwidth, and computing capability, than mobile nodes.

In EMA-RPL [22], the authors proposed RSSI-based mobility detection. Neighbouring static nodes are intimated about mobile nodes. Series of control messages transmitted from mobile node to neighbouring static node, and RSSI is calculated. A new preferred parent is determined based on the average RSSI. Though parent nodes can handle mobility on behalf of mobile nodes, an increasing number of mobile nodes may affect parent node performance in terms of data transmission latency, residual energy, and an increased number of control messages.

The authors suggested using LNR-PP [23], which uses RSSI-based mobility detection and leaf node count-based preferred parent selection, as suggested by the authors. Load balancing between parent nodes is taken into account.

Based on the literature survey, parent nodes are responsible for mobility detection and handling the handover process. The increment in the leaf node count burdens the parent node. Unbalanced loads on RPL degrade the performance of the network [24,25]. As a result, we highlight the need for a balanced mobile node allocation strategy that would preserve the performance of a parent node to some extent while increasing network availability.

4 BE-RPL: Terminologies, Control Packets, Timers

The terminology and timers associated with the proposed solution are explained in this section. Also included are the modifications made to the control packets. In the proposed solution, DODAG is made up of three types of nodes: the DODAG root node, the Stationary Node (SN), and the Mobile Node (MN). SNs are assumed to have a lot of resources. For MNs who are resource restricted, SNs act as preferred parents. The AMN Count (Associated Mobile Node Count) is the total number of MNs connected to the stationary node as leaf nodes.

The RSSI is a relative index value that represents the strength of the received signal. RSSI may be computed using Eq. (1):

$$\text{RSSI} = \text{Transmit Power} + \text{antenna gain} - \text{path loss} \tag{1}$$

Because the transmit power and antenna gain are constant for a given transmitter and receiver, and the path loss is proportional to the distance, RSSI may be stated as f (d). Then the distance will be f ′(RSSI). The RSSI can be used to discover the relative distance between a mobile node and its parent node. When RSSI is acceptable, it means the two nodes are getting closer. The value declines when MN creates some distance from its preferred parent.

4.1 Modification in ICMPv6 Control Messages

New fields have been added in the RPL defined ICMPv6 control messages. Fig. 1 depicts the IPv6 Internet Control Message Protocol. The kind of control message is determined by the code field.

- 0x00: DODAG Information Solicitation (DIS)
- 0x01: DODAG Information Object (DIO)
- 0x02: Destination Advertisement Object (DAO)
- 0x03: Destination Advertisement Object-Acknowledgment (DAO-ACK)

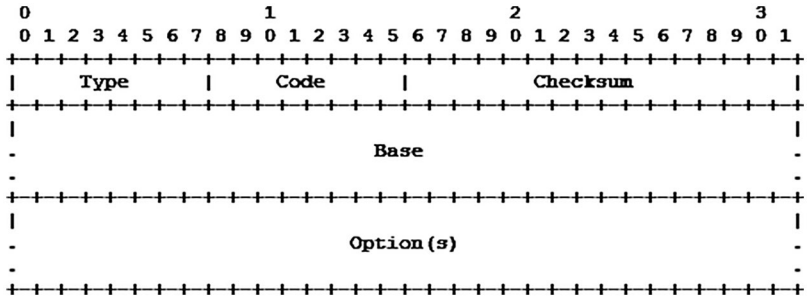

Figure 1: ICMPv6 control message format

BE-RPL modifies RPL-defined DIO and DIS control messages to aid the handover process. Fig. 2 depicts a DIO message that has been updated. The flag and RSSI fields have been added to the updated DIO message. Based on flag value, DIO messages are classified as DIO trickle timer, DIO-Attachment, and DIO-RSSI. Two bits make up the flag field. The RSSI field is made up of seven bits and is used by SN in the DIO-RSSI notification.

- If flag = 0x00, the message is a regular DIO message. Used to deliver a trickle timer notification on a regular basis.
- If flag = 0x01, the new PP node sends MN a DIO-Attachment notice message with the attachment data.

- If flag = 0x02, the neighbor SN will transmit a DIO-RSSI notification to the current PP node, which will contain the computed average RSSI and residual energy of the SN.

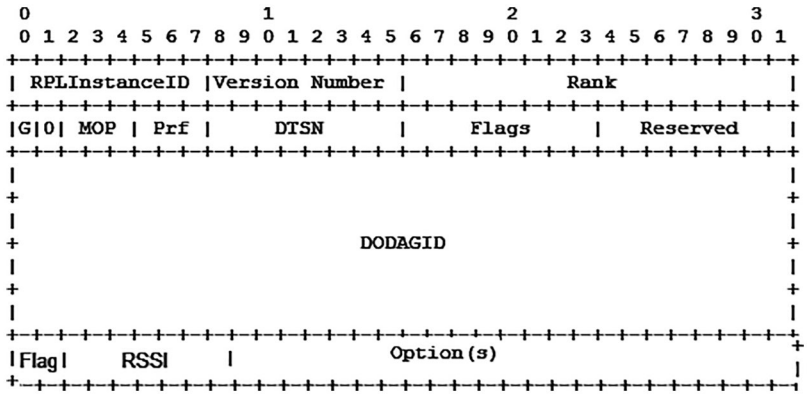

Figure 2: Modified DIO message

Fig. 3 depicts a modified DIS message format that includes two crucial fields: RSSI and MN-ID. The DIS message in RPL has an unused five-bit Flag field. DIS, DIS-Request, DIS-Burst, and DIS-Selection messages are classified using the flag value in BE-RPL.

- If flag = 0x00, the DIS message communicates solicitation information.
- If flag = 0x01: DIS-Request message. Current PP informs neighbour about mobility of MN and requesting to participate in election.
- If flag = 0x02: Used by MN to broadcast DIS-Burst messages.
- If flag = 0x03: DIS-Selection message. Current PP node notifies SN about its selection as the new PP node for MN.

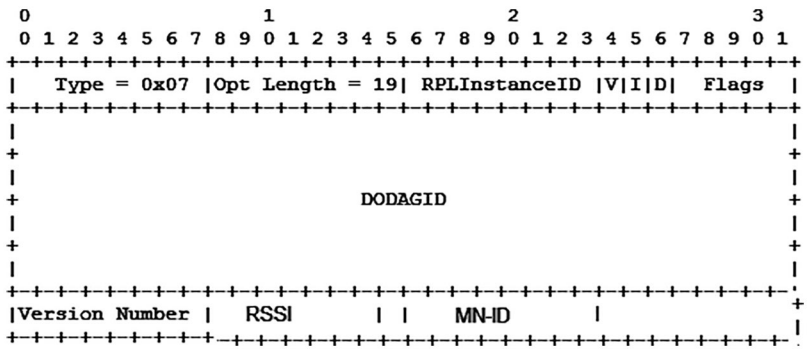

Figure 3: Modified DIS message

The RSSI field in the DIS-Request message contains seven bits of information that indicate the RSSI value between MN and the current PP node. The MN-ID field represents the mobile node's identification as it moves away from its PP node.

4.2 Timers

To make the transfer procedure easier, we included two timers.

After SN receives a DIS-Request and is willing to accommodate a new MN, it initialises the DIS-Delay timer. This is the waiting period to receive three DIS-Burst messages from MN.

When the parent node notifies MN about link deterioration, MN enables the DIS-Burst timer. It is equivalent to one-third of the DIS-Delay timer. MN broadcasts a DIS-Burst message for a DIS-Delay timer interval. After transmitting three DIS-Burst messages, MN disables this timer.

5 BE-RPL Protocol

MN first connects to the DODAG instance using RPL's default joining mechanism, and selects the preferred parent node. To identify node mobility and the accompanying handover procedure, the proposed protocol contains a mobility monitoring phase, an election phase, and an attachment phase.

The parent node monitors MN's movement using the RSSI value in the first stage. The election step for determining the new PP occurs when the node produces some distance from the PP. During the attachment phase, MN joins the freshly chosen PP as a leaf node and disconnects from the previous PP.

5.1 Mobility Monitoring Phase

The current PP node monitors the movement of each linked MN using RSSI. The quality of the link degrades as MN moves farther from the parent. The present PP node recognizes that MN is going away when RSSI is reduced to a predetermined value, Threshold 1 (TH1). The present PP node creates a DIS-Request packet with the flag value of one, MN-ID, and the latest RSSI value with moving MN as a consequence of this identification. TTL is transmitted as one. This ensures that the request is only processed by first-hop neighbors.

Until the new PP node is identified and connected, the current PP retains its connection with MN. Current PP nodes continue to receive data packets from MN until the value falls below Threshold 2. (TH2). MN is advised to stop sending data packets through the current PP node at that time. To identify movement, the trickle timer approach is not employed. To detect movement, no external signalling method is necessary. The phases of the mobility monitoring phase are depicted in Fig. 4.

5.2 Election Phase

The election stage is set when neighbors send DIS-Request messages. When a mobile node gets a DIS-Request message from PP, it performs the activities shown in Fig. 5. The MN node examines the RSSI value. If the value falls between TH1 and TH2, MN continues to deliver data packets to the current PP. Start the DIS-Burst timer with MN. MN sends out DIS-Burst signals per DIS-Burst interval. This DIS-Burst message has an MN ID and a flag value of two. MN sends out three DIS-Burst messages before turning off the timer. Due to the TTL value of one, only immediate neighbors process this packet.

If the RSSI value is less than TH2, it means that the MN node is approaching the end of its communication range with the current PP. To avoid data loss, it stops delivering data packets to the current PP node. The DIS-Burst clock is then triggered, and DIS-Burst messages are sent, as previously explained.

When SN receives a DIS-Request message, the steps are shown in Fig. 6. When a neighbor SN receives a DIS-Request message, they check to see how many attached MN they have. They reject the DIS-Request if it is attached with the most severe permissible count. They also reject the DIS-Burst signals sent by MN as a result. This cancellation of the request allows for load balancing amongst SNs.

The DIS-Request is acknowledged and the DIS-Delay timer is initiated if they are attached with a lesser number of MN. SN nodes must hang on in order to receive three DIS-Burst messages from MN. SN calculates the average RSSI after receiving DIS-Burst signals from MN.

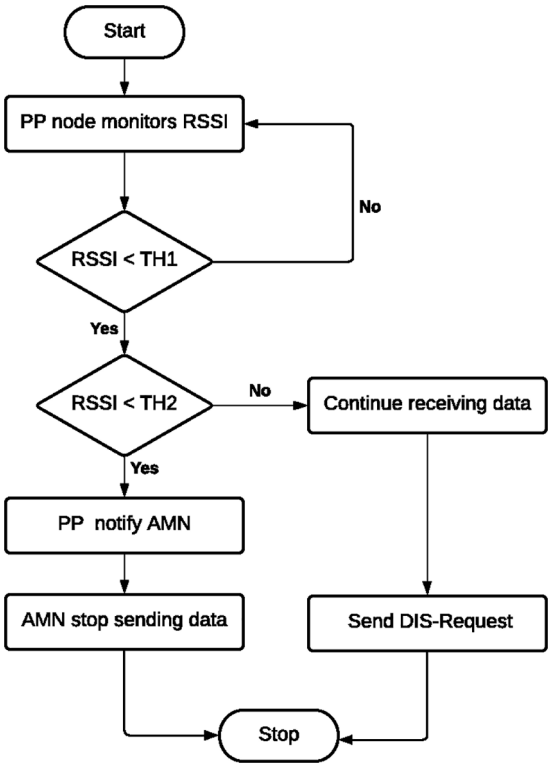

Figure 4: Mobility monitoring

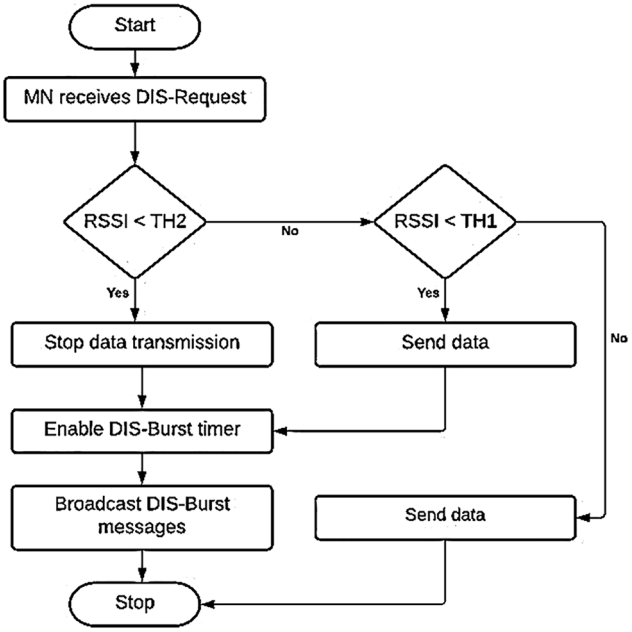

Figure 5: Election phase at mobile node

Average RSSI and the remaining energy of SN are intimated in unicast fashion using the DIO-RSSI message to the current PP which sent the DIS-Request.

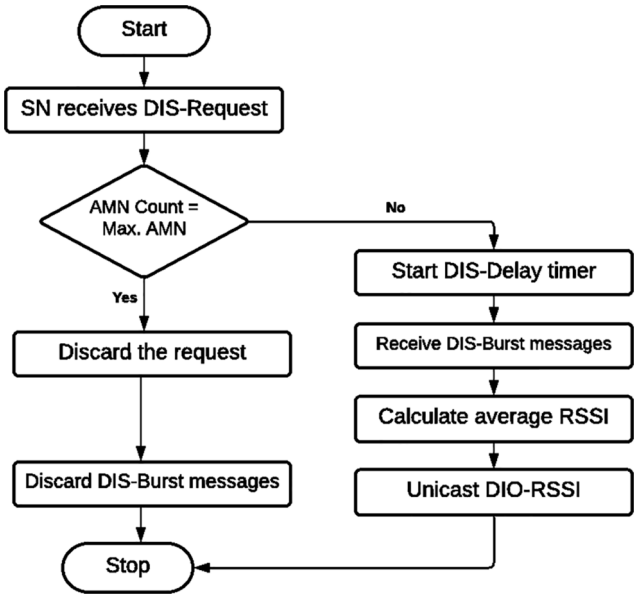

Figure 6: Election phase at static node

5.3 Attachment Phase

A new preferable parent is picked at the attachment step, and the route is updated. Fig. 7 depicts the attachment phase's flow.

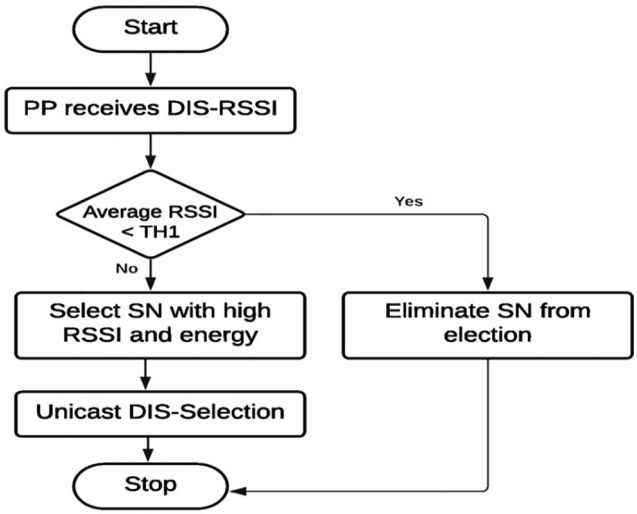

Figure 7: Attachment phase

DIO-RSSI messages are received by the present PP node from neighbouring SN nodes that are willing to accommodate MN. Nodes should have an average RSSI value greater than TH1 for the selection procedure. Based on SN's superior RSSI and residual energy, the current PP node picks the new preferred parent node. The present PP node sends a unicast DIS-Selection message to the chosen SN as notice. A selected SN sends a DIO message to MN after receiving a unicast DIS-Selection message.

MN updates its rank, PP node, and path to the root node. Two DAO messages were sent by MN. To recognize the connection, the first DAO message is unicasted to the new PP node. The second DAO was unicasted to the previous PP node for detachment. This ensures that MN is disconnected from the existing PP node after establishing a new connection with the new PP node. It aids in keeping the system away from data loss and connection disconnection.

6 Performance Evaluation

To evaluate the proposed BE-RPL's performance and compare it to standard RPL and EMA-RPL, we simulated it. The BE-RPL is analyzed on the Contiki-NG platform with the help of the COOJA simulator. In contrast to previous simulators, COOJA allows concurrent simulation at several levels by merging low-level hardware simulation with high-level behavior modeling in a single simulation. The primary reasons for using Contiki are the availability of a widely used RPL implementation and the existence of a mobility plugin in COOJA.

6.1 Simulation Setup

RPL-LITE and RPL-CLASSIC versions are supported by Contiki-NG. For analysis, RPL CLASSIC is used. Simulation has been chosen for the Unit Disk Graph Model (UDGM) with distance loss system. For simulation, Zolertia Z1 motes were chosen. The Energest module is enabled to determine how much energy each mote uses. The random walk model mobility extension will now be included and implemented.

For comparing BE-RPL with EMA-RPL, both are implemented using Contiki RPL_CLASSIC. Different scenarios are simulated depending on the number of mobile nodes. The SNs are arranged in a linear grid. We look at energy usage, packet delivery ratio, and packet overhead management in all cases.

Tab. 1 lists the simulation parameters that are used for the COOJA simulation.

Table 1: Simulation parameters

Simulation area	200 m × 200 m
Simulation time	3600 s
No. of static nodes	10
No. of mobile nodes	1, 2, 3, 4, 5
Traffic type	CBR
Transceiver ratio	Tx = 100%, Rx = 100%
Mobility model	Random walk model
RSSI	TH1: −83 dBm, TH2: −92 dBm
Timer	DIS-Burst timer: 20 ms DIS-Delay timer: 60 ms

The COOJA simulation with five mobile nodes is shown in Fig. 8. The transmission range and interference range are both set to 50 and 100 m. It also displays how nodes are connected to one another.

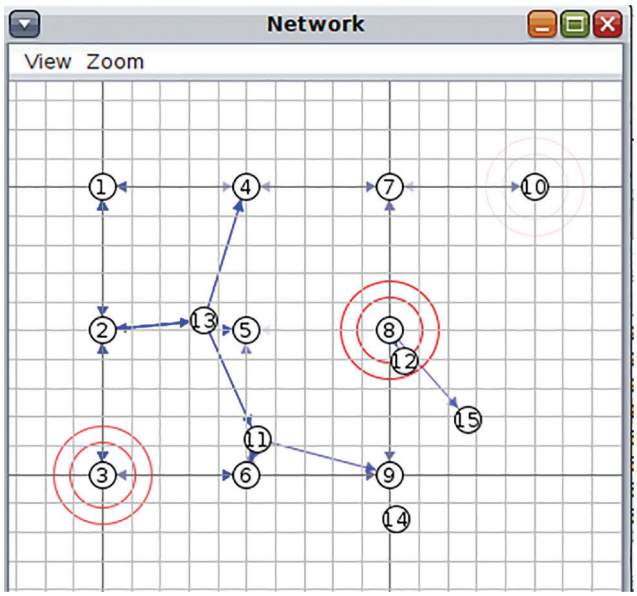

Figure 8: COOJA simulation with five mobile nodes

6.2 Control Overhead

In this section, we compare the BE-RPL protocol's network control overhead to that of the EMA-RPL protocol and regular RPL. The network control overhead refers to the total number of packets sent in signalling messages to assist connection setup, mobility, and data transmission (ICMPv6 messages). BE-RPL's main purpose is to create seamless, continuous communication while conserving energy. It is vital to minimise the cost of signalling in order to attain this aim. Because no extra signalling is required, the RPL protocol obviously has the lowest signalling cost. When compared to BE-RPL and regular RPL, EMA-RPL has a higher control overhead. When the number of exchanged control messages between the MN and its preferred parent is lowered in BE-RPL, the network is relieved, enabling more data packets to be delivered. In all circumstances, the cost of signalling is much lower than with EMA-RPL, as shown in the diagram. Eq. (2) calculates the total amount of network control overhead as the sum of all DIO, DIS, DAO, and DAO-ACK messages.

$$\text{Network control overhead} = \Sigma\,\text{DIO} + \Sigma\,\text{DIS} + \Sigma\,\text{DAO} + \Sigma\,\text{DAO} - \text{ACK} \tag{2}$$

Fig. 9 clearly indicates that in the single mobile node situation, network control overhead is lower for all protocols. When mobile nodes are put together, network overhead increases across all routing methods. By excluding heavily loaded nodes from the election phase, BE-RPL decreases the amount of DIO-RSSI broadcasts.

6.3 Energy Consumption

Low-power devices have a number of challenges, the most significant of which is energy consumption. The energy monitoring module assesses the CPU energy consumption in active, low power, and deep low power modes. It additionally screens the energy usage of the radio transceiver in transmission and receiving mode.

The CC2420 radio transceiver is used by the Zolertia Z1 mote. At 3 V, this mote uses 17.4 mA for transmission and 19.7 mA for reception [26]. The Energest module provides energy consumption details indirectly [27]. It shows the time spent in each state of the transceiver. For the CC2420 transceiver, ticks

per second for real time are 32770. It is denoted as RTIMER_SECOND. Time spent, current, and voltage at a certain state are used to calculate the energy consumed at that state. For example, Eq. (3) gives the amount of energy consumed during the transmission state.

$$E_{TX} = \frac{I_{TX} * \ V_{TX} * \text{Energest} \ \ \text{value}_{TX}}{\text{RTIMER\_SECOND}} \tag{3}$$

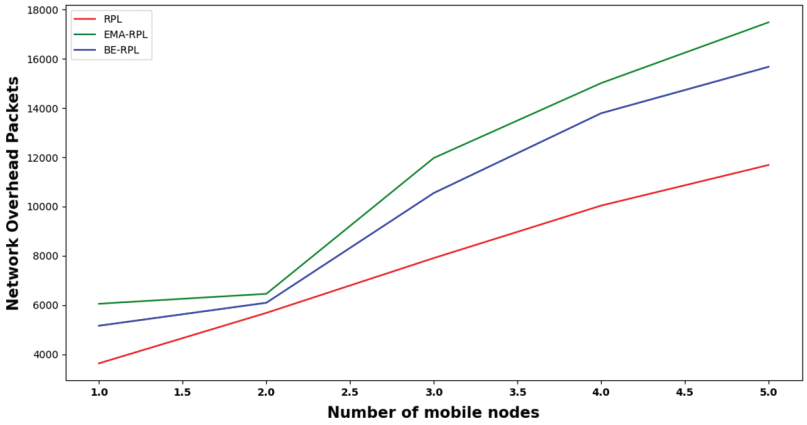

Figure 9: Network control packets overhead

In Eq. (4), the total energy used is computed by adding the energy consumed in all states.

$$E = \ E_{TX} + E_{RX} + E_{LPM} + \ E_{DPLM} + E_{CPU} \tag{4}$$

The output of the mote's Energest module is shown in Fig. 10.

Fig. 11 shows how energy consumption varies depending on the number of mobile nodes. As seen in the figure, an increase in MN is unavoidably accompanied by an increase in energy consumption. Because of the lower control overhead, the conventional RPL uses less energy than the EMA-RPL and BE-RPL. Only qualified SNs are permitted to process the DIS-Request and vote in the election. It conserves energy by ensuring nodes have a minimum remaining power. The reduction in energy use was a direct result of this development. As a consequence, BE-RPL performs better than EMA-RPL.

6.4 Packet Delivery Ratio

We calculate the PDR of the standard RPL, EMA-RPL, and BE-RPL to induce network reliability. Static nodes get 100% PDR in all cases. Mobile nodes have less PDR. For RPL, EMA-RPL, and BE-RPL, a single mobile node achieves 60%, 80.17%, and 84.34% packet delivery ratios, respectively as shown in Fig. 12. BE-RPL provides good route stability by reducing the number of link breakdowns. It improves the packet delivery ratio.

The average end-to-end packet delivery ratio for all five scenarios is shown in Fig. 13. BE-RPL can achieve 90.29% end-to-end PDR in a scenario with five mobile nodes. Both EMA-RPL and regular RPL reach 89.14% and 85.61%, respectively, for the same case. BE-RPL outperforms EMA-RPL in terms of PDR due to MN's rapid attachment to the new preferred parent. The BE-RPL is successful because it addresses load balancing among SNs. The BE-RPL network appears to be more reliable than the EMA-RPL and regular RPL networks.

Time	Mote	Message
04:01.371	ID:9	[INFO: Energest] Deep LPM : 0/ 1966080 (0 permil)
04:01.374	ID:26	[INFO: Energest] --- Period summary #3 (59 seconds)
04:01.378	ID:9	[INFO: Energest] Radio Tx : 167/ 1966080 (0 permil)
04:01.378	ID:26	[INFO: Energest] Total time : 1966079
04:01.381	ID:10	[INFO: Energest] --- Period summary #3 (60 seconds)
04:01.384	ID:26	[INFO: Energest] CPU : 13083/ 1966079 (6 permil)
04:01.385	ID:9	[INFO: Energest] Radio Rx : 1965912/ 1966080 (999 permil)
04:01.385	ID:10	[INFO: Energest] Total time : 1966080
04:01.386	ID:6	[INFO: Energest] --- Period summary #3 (60 seconds)
04:01.390	ID:6	[INFO: Energest] Total time : 1966080
04:01.391	ID:26	[INFO: Energest] LPM : 1952996/ 1966079 (993 permil)
04:01.392	ID:10	[INFO: Energest] CPU : 54284/ 1966080 (27 permil)
04:01.392	ID:9	[INFO: Energest] Radio total : 1966079/ 1966080 (999 permil)
04:01.396	ID:6	[INFO: Energest] CPU : 37941/ 1966080 (19 permil)
04:01.397	ID:26	[INFO: Energest] Deep LPM : 0/ 1966079 (0 permil)
04:01.399	ID:10	[INFO: Energest] LPM : 1911796/ 1966080 (972 permil)
04:01.404	ID:26	[INFO: Energest] Radio Tx : 166/ 1966079 (0 permil)
04:01.404	ID:6	[INFO: Energest] LPM : 1928139/ 1966080 (980 permil)
04:01.405	ID:10	[INFO: Energest] Deep LPM : 0/ 1966080 (0 permil)
04:01.410	ID:6	[INFO: Energest] Deep LPM : 0/ 1966080 (0 permil)
04:01.411	ID:26	[INFO: Energest] Radio Rx : 1965911/ 1966079 (999 permil)
04:01.411	ID:10	[INFO: Energest] Radio Tx : 1146/ 1966080 (0 permil)
04:01.416	ID:6	[INFO: Energest] Radio Tx : 1018/ 1966080 (0 permil)
04:01.418	ID:26	[INFO: Energest] Radio total : 1966077/ 1966079 (999 permil)
04:01.418	ID:10	[INFO: Energest] Radio Rx : 1964918/ 1966080 (999 permil)
04:01.423	ID:6	[INFO: Energest] Radio Rx : 1965048/ 1966080 (999 permil)
04:01.426	ID:10	[INFO: Energest] Radio total : 1966064/ 1966080 (999 permil)
04:01.430	ID:6	[INFO: Energest] Radio total : 1966066/ 1966080 (999 permil)
04:01.447	ID:22	[INFO: Energest] --- Period summary #3 (59 seconds)
04:01.451	ID:22	[INFO: Energest] Total time : 1966079
04:01.458	ID:22	[INFO: Energest] CPU : 17876/ 1966079 (9 permil)
04:01.465	ID:22	[INFO: Energest] LPM : 1948203/ 1966079 (990 permil)
04:01.471	ID:22	[INFO: Energest] Deep LPM : 0/ 1966079 (0 permil)
04:01.477	ID:22	[INFO: Energest] Radio Tx : 453/ 1966079 (0 permil)
04:01.484	ID:22	[INFO: Energest] Radio Rx : 1965621/ 1966079 (999 permil)

Figure 10: Mote output

6.5 Frame Acknowledgement Ratio

A frame delivered with the acknowledgement request field set to 1 must be acknowledged by the receiver. If the frame is successfully received, the intended receiver must create and send an acknowledgement frame with the same DSN as the data or MAC command frame being acknowledged. The acknowledgement must be provided between aTurnaroundTime and aTurnaroundTime + aUnitBackoffPeriod symbols after receiving the final symbol of the data or MAC command frame. The frame acknowledgement ratio is calculated using Eq. (5).

$$\text{Frame acknowledgement ratio} = \text{ll\_par} = 100.0 * \text{total\_ll\_acked} / \text{total\_ll\_sent} \quad (5)$$

When standard RPL is used as a routing protocol, the frame acknowledgment ratio is lower in all circumstances (see Fig. 14). In normal RPL, more frames are lost due to frequent link breaks. By preventing link breaks, BE-RPL considerably boosts FAR.

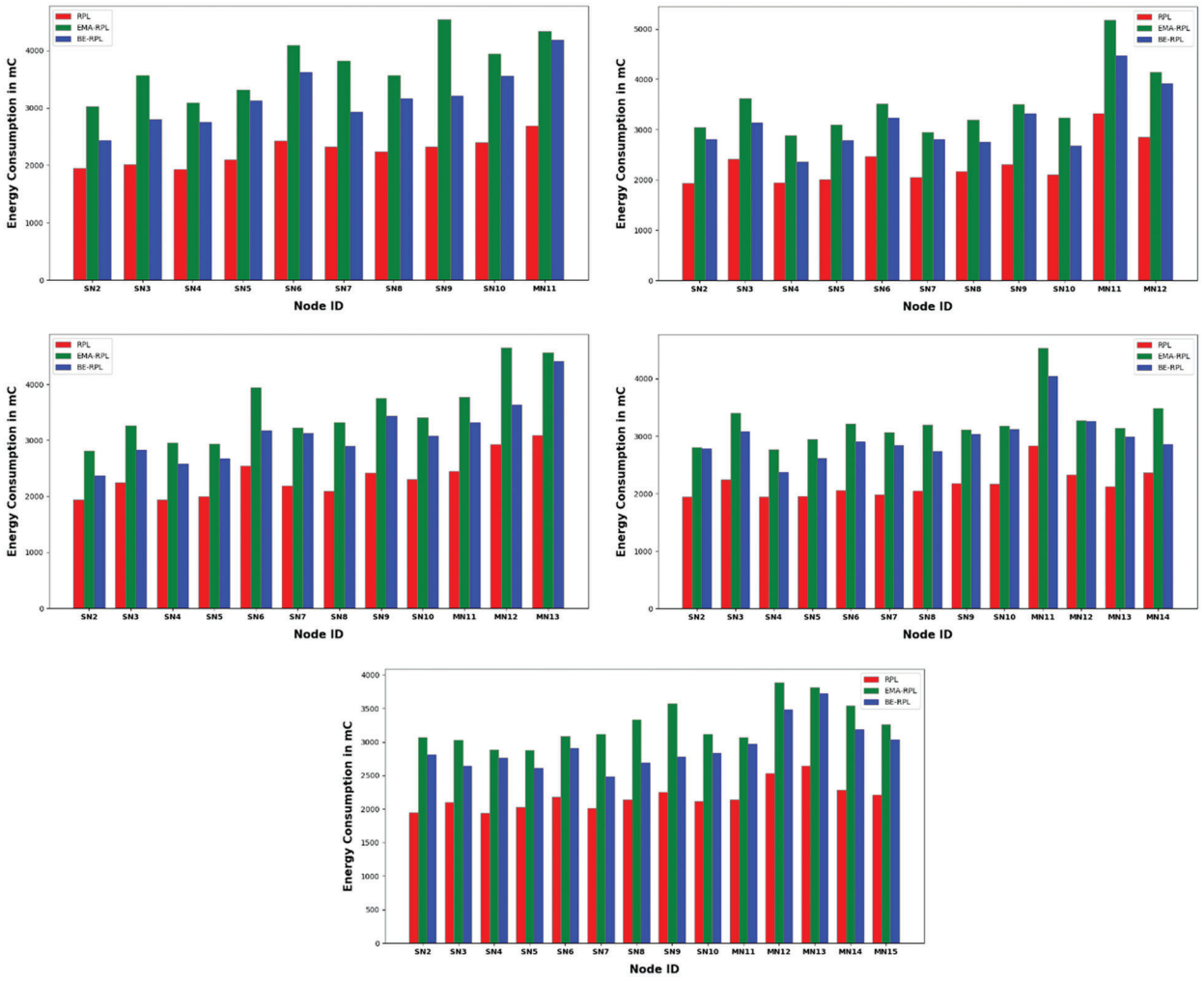

Figure 11: Energy consumption for different scenario

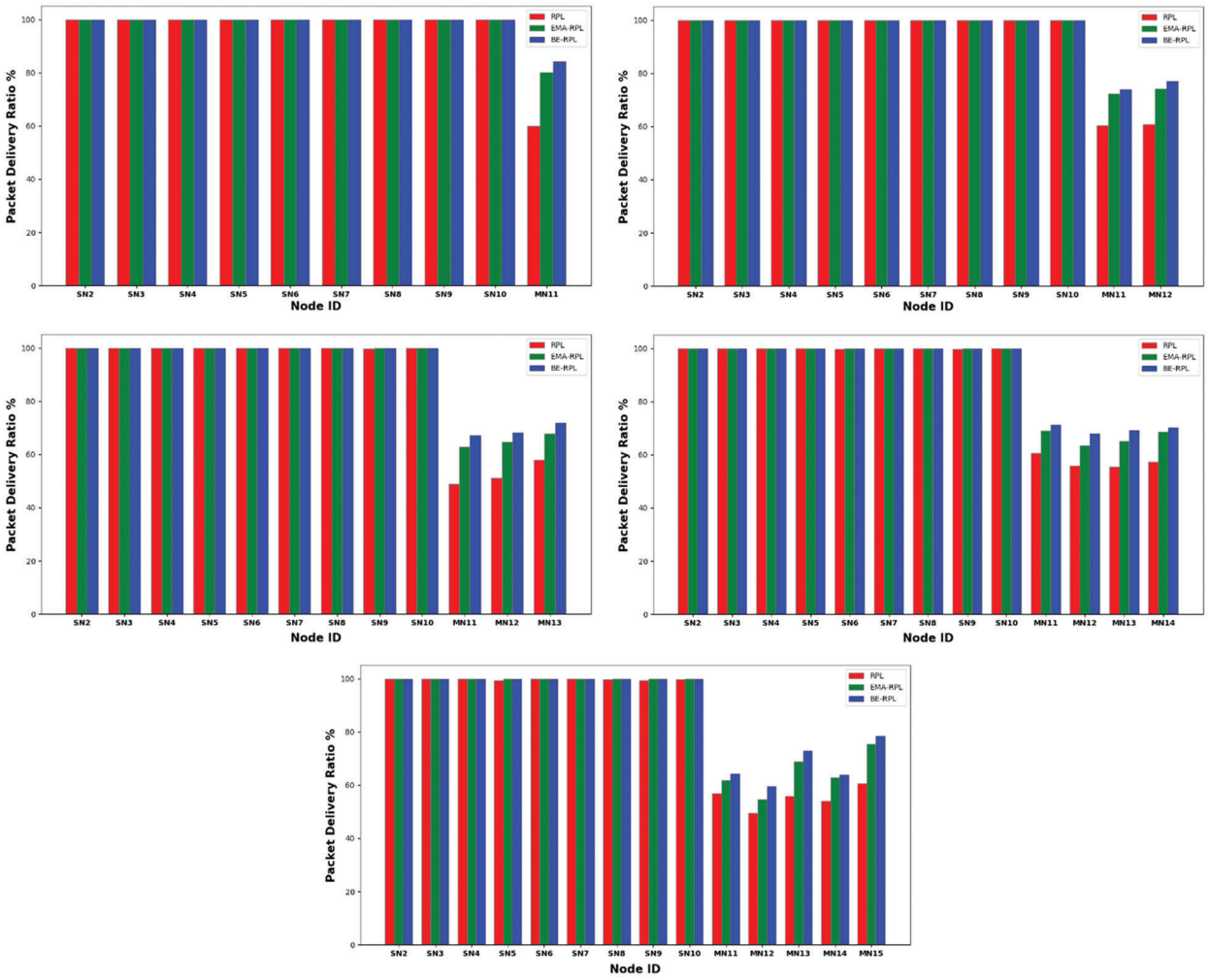

Figure 12: PDR for different scenario

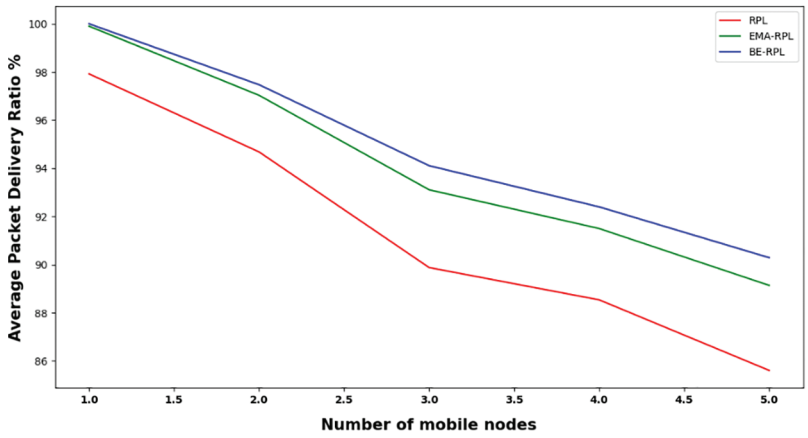

Figure 13: Average end-to-end PDR for different scenario

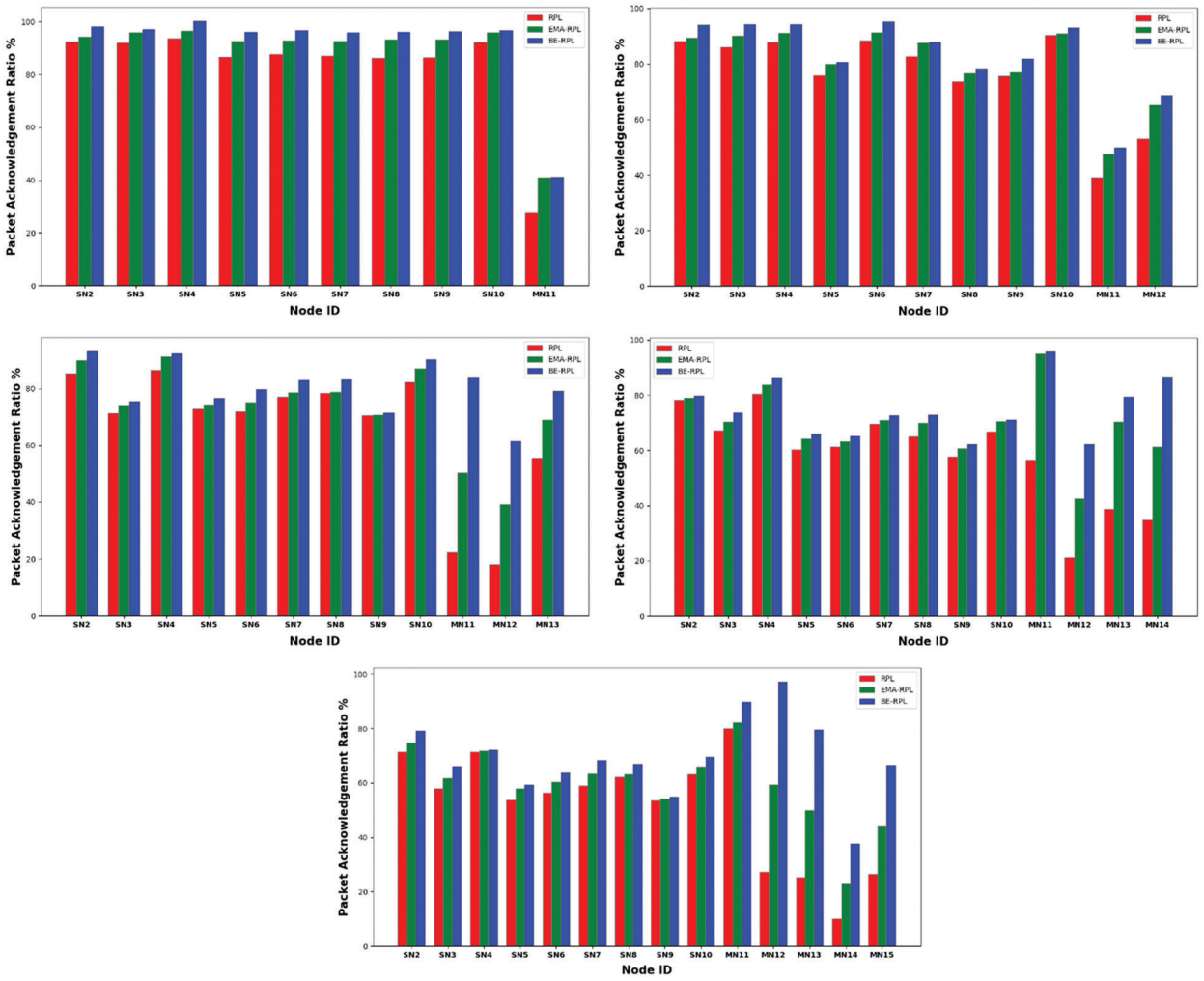

Figure 14: FAR for all five scenarios

7 Conclusion

To address micro-mobility on the Internet of Things, we suggested BE-RPL, a suitable protocol for real-time applications. In RPL, we highlighted the problem of mobile nodes and proposed BE-RPL as a best-effort approach to assign balanced mobile nodes to SN. It ensures constant, smooth connectivity and makes mobile nodes reachable regardless of their location. BE-RPL is a proactive technique that predicts mobility based on RSSI. A MN chooses a new favorite parent based on the average RSSI and attached mobile node count. We used timers to improve hand-off efficiency by lowering hand-off delays and network congestion.

Extensive simulations and experiments were employed to test, fine-tune, and validate the BE-RPL integration using Contiki-NG. According to simulation findings, BE-RPL provides dependable mobility support for the RPL protocol. When compared, the BE-RPL outperforms both the original RPL and the EMA-RPL.

Funding Statement: The authors received no specific funding for this study.

Conflicts of Interest: The authors declare that they have no conflicts of interest to report regarding the present study.

References

[1] Q. M. Ashraf and M. H. Habaebi, "Autonomic schemes for threat mitigation in internet of things," *Journal of Network and Computer Applications*, vol. 49, pp. 112–127, 2015.

[2] M. Roopa and S. Selvakumar Raja, "Intelligent intrusion detection and prevention system using smart multi-instance multi-label learning protocol for tactical mobile adhoc networks," *KSII Transactions on Internet and Information Systems (TIIS)*, vol. 12, no. 6, pp. 2895–2921, 2018.

[3] M. Roopa and S. Selvakumar Raja, "An intelligent network algorithm for enhanced security in a mobile ad hoc network," *International Journal of Networking and Virtual Organisations*, vol. 17, no. 2–3, pp. 126–136, 2017.

[4] P. D. Acevedo, D. Jabba, P. Sanmartín and S. Valle, "WRF-RPL: Weighted random forward RPL for high traffic and energy demanding scenarios," *IEEE Access*, vol. 9, pp. 163–174, 2017.

[5] M. Amirinasab Nasab, S. Shamshirband, A. T. Chronopoulos and A. Mosavi, "Energy-efficient method for wireless sensor networks low-power radio operation in internet of things," *Electronics*, vol. 9, no. 2, Article ID 320, 2020.

[6] F. A. Almalki, S. B. Othman, F. A. Almalki and H. Sakli, "EERP-DPM: Energy efficient routing protocol using dual prediction model for healthcare using IoT," *Journal of Healthcare Engineering*, vol. 2021, pp. 1–15, 2021.

[7] A. Y. Barnawi, G. A. Mohsen and E. Q. Shahra, "Performance analysis of RPL protocol for data gathering applications in wireless sensor networks," *Procedia Computer Science*, vol. 151, pp. 185–193, 2019.

[8] U. Khan, I. M. Qureshi, M. A. Aziz, T. A. Cheema and S. B. H. Shah, "Smart IoT control-based nature inspired energy efficient routing protocol for flying ad Hoc network (FANET)," *IEEE Access*, vol. 8, pp. 56371–56378, 2020.

[9] I. U. Khan, M. A. Hassan and M. D. Alshehri, "Monitoring system-based flying IoT in public health and sports using ant-enabled energy-aware routing," *Journal of Healthcare Engineering*, vol. 2021, Article ID 1686946, pp. 11, 2021.

[10] M. A. Lodhi, A. Rehman, M. M. Khan, M. Asfand-e-yar and F. B. Hussain, "Transient multipath routing protocol for low power and lossy networks," *KSII Transactions on Internet and Information Systems (TIIS)*, vol. 11, no. 4, pp. 2002–2019, 2017.

[11] A. Triantafyllou, P. Sarigiannidis and T. D. Lagkas, "Network protocols, schemes, and mechanisms for internet of things (IoT): Features, open challenges, and trends," *Wireless Communications and Mobile Computing*, vol. 2018, Article ID 5349894, pp. 24, 2018.

[12] B. Safaei, A. A. M. Salehi, A. M. H. Monazzah and A. Ejlali, "Effects of RPL objective functions on the primitive characteristics of mobile and static IoT infrastructures," *Microprocessors and Microsystems*, vol. 69, pp. 79–91, 2019.

[13] M. Pushpalatha, T. Anusha, T. R. Rao and R. Venkataraman, "L-RPL: RPL powered by laplacian energy for stable path selection during link failures in an internet of things network," *Computer Networks*, vol. 184, Article ID 107697, 2021.

[14] X. Niu, "Optimizing DODAG build with RPL protocol," *Mathematical Problems in Engineering*, vol. 2021, Article ID 5579564, pp. 8, 2021.

[15] T. Winter, P. Thubert, A. Brandt and J. P. Vasseur, "RPL: IPv6 routing protocol for low-power and lossy networks," vol. rfc 6550, pp. 1–157, 2012.

[16] H. Lamaazi and N. Benamar, "A novel approach for RPL assessment based on the objective function and trickle optimizations," *Wireless Communications and Mobile Computing*, vol. 2019, Article ID 4605095, pp. 9, 2019.

[17] K. Srisomboon, T. Dindam and W. Lee, "Empowered hybrid parent selection for improving network lifetime, PDR, and latency in smart grid," *Mathematical Problems in Engineering*, vol. 2021, Article ID 5551152, pp. 19, 2021.

[18] K. C. Lee, R. Sudhaakar, J. Ning, L. Dai, S. Addepalli *et al.,* "A comprehensive evaluation of RPL under mobility," *International Journal of Vehicular Technology*, vol. 2012, Article ID 904308, pp. 10, 2012.

[19] Tian Bin, Kun Mean Hou, Hongling Shi, Xing Liu, Xunxing Diao et al., "Application of modified RPL under VANET-WSN communication architecture," *2013 international conference on computational and information sciences*, IEEE, pp. 1467–1470, 2013.

[20] I. El Korbi, M. B. Brahim, C. Adjih and L. A. Saidane, "Mobility enhanced RPL for wireless sensor networks," in *2012 Third Int. Conf. on the Network of the Future (NOF)*, IEEE, pp. 1–8, 2012.

[21] F. Hossein, D. Moreira and M. Alves, "mRPL: Boosting mobility in the internet of things," *Ad Hoc Networks*, vol. 26, pp. 17–35, 2015.

[22] B. Maha, A. Rachedi, A. Belghith, M. Berbineau and S. Al-Ahmadi, "EMA-RPL: Energy and mobility aware routing for the internet of mobile things," *Future Generation Computer Systems*, vol. 97, pp. 247–258, 2019.

[23] P. Suganya and C. H. Pradeep Reddy, "LNR-PP: Leaf node count and RSSI based parent prediction scheme to support QoS in presence of mobility in 6LoWPAN," *Computer Communications*, vol. 150, pp. 472–487, 2020.

[24] A. Seyfollahi and A. Ghaffari, "A lightweight load balancing and route minimizing solution for routing protocol for low-power and lossy networks," *Computer Networks*, vol. 179, Article ID 107368, 2020.

[25] D. Pancaroglu and S. Sen, "Load balancing for RPL-based internet of things: A review," *Ad Hoc Networks*, vol. 116, Article ID 102491, 2021.

[26] K. Kritsis, G. Z. Papadopoulos, A. Gallais, P. Chatzimisios and F. Theoleyre, "A tutorial on performance evaluation and validation methodology for low-power and lossy networks," *IEEE Communications Surveys & Tutorials*, vol. 20, no. 3, pp. 1799–1825, 2018.

[27] A. Sabovic, C. Delgado, J. Bauwens, E. D. Poorter and J. Famaey, "Accurate online energy consumption estimation of IoT devices using energest," in *Int. Conf. on Broadband and Wireless Computing, Communication and Applications*, Cham, Springer, pp. 363–373, 2019.